

Quenching of metal sticking by photo-oxidation of an amorphous semiconductor: Zn on GeS₂

J. Hugh Horton, Christopher Hardacre, Christopher J. Baddeley, Geoffrey D. Moggridge, R. Mark Ormerod,* and Richard M. Lambert[†]

Department of Chemistry, University of Cambridge, Lensfield Road, Cambridge CB2 1EW, United Kingdom

(Received 19 August 1994)

The sticking probability of Zn on amorphous GeS₂ is greatly reduced when the UHV-prepared semiconductor film is photo-oxidized in the presence of band-gap radiation. The phenomena underlying this interesting effect have been elucidated in a kinetic and structural study using electron spectroscopy and x-ray-absorption spectroscopy. Selective photo-oxidation of Ge sites strongly suppresses the formation of Ge-Zn bonds at the interface: these act as nucleation sites for the growing metal film. A consistent picture emerges that also accounts for the very different behavior encountered during deposition of Ag films with and without photo-oxidation in the closely related Ag/GeS₂ system.

I. INTRODUCTION

Chalcogenide vitreous semiconductors (CVS) such as GeS₂ exhibit a number of interesting and potentially useful photoeffects. While some of these, such as photodiffusion of Ag or Zn (Ref. 1) and photodarkening (Ref. 2) have long been recognized, an effect in which the sticking probability of vapor phase Zn metal on a CVS is strongly influenced by pretreatment of surface has only been more recently discovered.^{1,3,4} Specifically, it has been found that irradiation of GeS₂ or As₂S₃ thin films with band-gap light in the presence of O₂ (photo-oxidation) can reduce the initial sticking coefficient of Zn by several orders of magnitude. Interestingly, the sticking probability of other metals on the photo-oxidized films is unaffected. A preliminary x-ray-photoelectron spectroscopy (XPS) investigation of this effect,⁵ using As₂S₃ films prepared *ex situ* showed that irradiation of the films in air leads to preferential oxidation of the As sites. Much more controlled *in situ* studies, using Auger-electron spectroscopy (AES) and XPS under UHV conditions,^{6,7} on the photo-oxidation of GeS₂ in O₂ have shown that in this case, the Ge sites are indeed preferentially oxidized. This implies that the nonchalcogenide site is crucial in the subsequent nucleation of Zn on the surface and that the Zn preferentially sticks to the Ge sites. Preferential oxidation of the nonchalcogenide site is analogous to the recently reported preferential chlorination of Ga sites on GaAs (110).⁸ Previous studies of Zn deposition of CVS surfaces used a quartz-crystal thickness monitor to determine the amount of Zn deposited;⁴ these demonstrated that the phenomenon is characterized by an induction period of low sticking probability, which occurs over less than the first 5 Å of Zn deposition. Subsequently, the deposition rate was increased by a factor of 50–200 times, dependent on the extent of preexposure to illumination and O₂; sticking probability effects were seen even on films which had not been photo-oxidized. While these experiments were an important demonstration of the effect, they suffered from a number of limitations. First, vacuum conditions were poorly controlled, with

pressures on the order of 10⁻⁶ torr and with breaks in vacuum between the CVS deposition, photo-oxidation and Zn deposition stages of the experiment, leading to possible contamination of the film surface. Second, the gravimetric technique used gives no information on the chemical identity of the Zn overlayers, their extent of reaction with the substrate, or of the growth mode.

Here, we present the results of a rigorous study of Zn deposition on amorphous GeS₂ films using a combination of laboratory/UHV surface science and synchrotron x-ray-absorption spectroscopy methods. Growth modes on clean and photo-oxidized surfaces were examined using AES, while the metal-substrate interaction was studied by XPS and x-ray excited Auger-electron spectroscopy (XAES). In addition, the “inverse” system, i.e., GeS₂ deposition on Zn, was examined using the same techniques. Using these methods we have also prepared layered GeS₂/Zn sample for a structural study of the metal/CVS interface using extended x-ray-absorption fine structure (EXAFS). The results are discussed with reference to mechanisms for the sticking probability effect and are also compared to those found for an important photodiffusion system: Ag-GeS₂.^{1,6,9} In particular, we show that the possibility of metal-sulfur or metal-germanium bonding has important consequences in the subsequent nucleation and growth characteristics of the metal overlayer.

II. EXPERIMENT

Experiments were carried out in two UHV chambers, which have been previously described.^{6,10} Both were equipped with a high-pressure cell/transfer system for preparation of the photo-oxidized films; in chamber A the high-pressure cell could also double as an airlock. Base pressures of 1×10⁻¹⁰ torr or better could be routinely achieved on both chambers. Chamber A was equipped with standard UHV techniques: a retarding field analyzer (RFA) for AES measurements; Ar-ion cleaning; and mass spectrometer for residual gas analysis. Chamber B was also equipped with standard techniques including ion gun, mass spectrometer, and a VSW

HA100 spectrometer system for XPS/AES analysis. Al $K\alpha$ radiation was used for acquiring XP spectra, which were referenced to the valence-band cutoff, and to the Ni $2p_{3/2}$ peak (632.9 eV) from the Ni substrate. Both chambers were equipped with GeS_2 and Zn thermal evaporation sources. The operation and deposition characteristics of the GeS_2 source have been previously described.¹¹ The Zn source was water cooled to prevent metal evaporation during bakeout; the water cooling was turned off during normal operation of the source. During operation of either source, the chamber pressure remained below 5×10^{-10} torr. Analysis of the deposited Zn showed no evidence for contamination as judged from the AES signal.

The GeS_2 substrates required for Zn deposition experiments were grown on Ni foil. These were about 80 Å thick and have been previously characterized in detail.^{9,11} Photo-oxidation of the films took place in the high-pressure cell, and preparation methods and characteristics of the photo-oxidized films have also been previously described.^{6,7} Samples underwent various degrees of photo-oxidation in these experiments: those films subsequently referred to as "partially photo-oxidized" had about half a monolayer of oxide coverage on the surface; those referred to as "fully photo-oxidized" were photo-oxidized to the saturation point. In this latter case, several layers of oxidized GeS_2 have been formed.

A layered Zn/ GeS_2 sample was prepared in order to increase substantially the signal to noise ratio of our EXAFS experiments. It contained 12 GeS_2/Zn interfaces prepared in chamber *A* under UHV conditions. Calibration of the deposited layer thicknesses was carried out using AES and the sample characteristics are summarized below.

(1) GeS_2 deposited on Ni foil substrate for 1 h (approx. 40 Å); (2) Zn deposited for 30 min (approx. 10 Å); (3) GeS_2 deposited for 20 min (approx. 12 Å), steps 2 and 3 repeated a total of six times; (4) GeS_2 deposited for 1 h (approx. 40 Å). Once the sample was completed, it was transferred out of chamber *A* via the high-pressure cell/airlock to a dessicator where it was shielded from ambient light during storage and transfer to the synchrotron. EXAFS experiments were carried out on the sample at the Ge and Zn K edges at station 9.3, Daresbury Synchrotron Laboratory. Experiments were performed in a fluorescence mode under ambient conditions. Two standards were also run, both in transmission mode, as follows. A 10 μm Zn foil was placed directly in the beam to act as a Zn standard. A ZnS standard was run by grinding ZnS powder with BN. The mixture was placed in a cell with Be windows, which was also placed directly in the beam. Background subtraction of the EXAFS spectra was carried out, using the EXCALIB and EXBROOK programs available on the Daresbury Convex system. The spectra were fitted using the program EXCURV92 (Ref. 12) also on the Daresbury Convex.

III. RESULTS

A. Zn deposition on GeS_2

Zinc deposition experiments were initially carried out in chamber *A* at 300 K. In Fig. 1, the Zn $M_{2,3}M_{4,5}M_{4,5}$,

S $LM_{2,3}M_{2,3}$, and Ge M_1M_3V Auger signals are plotted as a function of Zn deposition time on an as-deposited GeS_2 film and two films, which had previously undergone different degrees of photo-oxidation. Several features should be immediately noted: first, on the clean GeS_2 film, a distinct break point is observed at 10 min deposition time in the Zn uptake data. This break point provides a convenient calibration for the source deposition rate and in the following discussion will be referred to as the monolayer point. Over the same time, the S signal has attenuated to 70% of its initial value, while the Ge signal is almost completely quenched. The apparent slight recovery in the Ge signal at about 20 min deposition time can be attributed to interference from a minor Zn Auger transition at ≈ 50 eV. Second, on the photo-oxidized surfaces a distinct induction period before the onset of Zn deposition is observed. This is characterized by little or no Zn signal being detected for the first 10–20 min of deposition time; over the same period, no apparent decrease in the S or Ge signals is observed. After the induction period is complete, changes in the subsequent growth mode are observed on the heavily photo-oxidized substrate.

Further experiments on Zn deposition, using XPS, and XAES were carried out in chamber *B*. Calibration of the Zn source in this chamber indicated that in this case, the break in the Zn AES uptake curve occurred at 40 min deposition time (the S AES signal underwent a similar degree of attenuation at this point as in chamber *A*). Thus, it is important to note that in the following Figs. 2–4 the deposition times indicated correspond to a deposition rate $\frac{1}{4}$ of that observed in Fig. 1. Figure 2 shows the Zn $L_3M_{4,5}M_{4,5}$ XAES signal as a function of Zn deposition

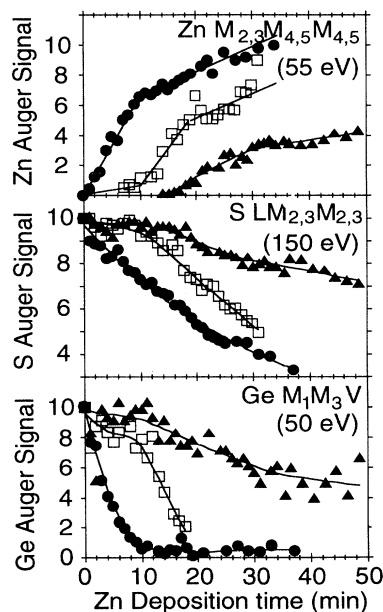


FIG. 1. The Zn, S, and Ge peak-to-peak heights (in arbitrary units) as a function of Zn deposition time on various GeS_2 substrates. Closed circles: clean (as deposited) GeS_2 ; open squares: partially photo-oxidized substrate; closed triangles: substrate photo-oxidized to saturation point.

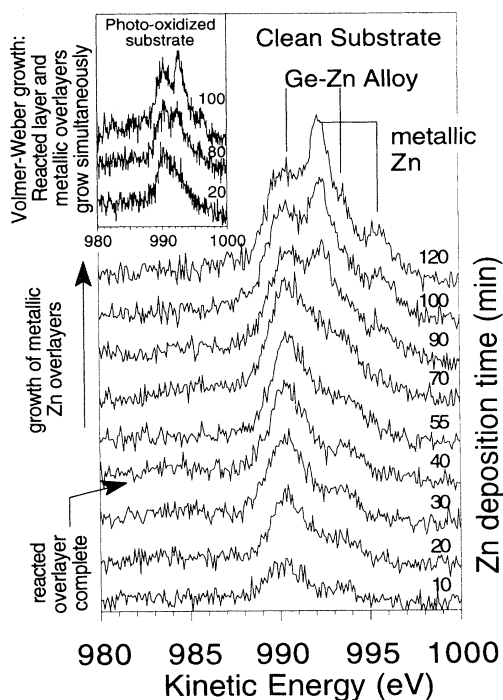


FIG. 2. The Zn $L_3M_{4.5}M_{4.5}$ XAES spectrum as a function of Zn deposition time on clean GeS_2 (main figure) and on a GeS_2 film photo-oxidized to the saturation point (inset). The Zn deposition rate in this case was $0.25\times$ that of the experiment in Fig. 1. Thus, a deposition time of 40 min here corresponds to a deposition time of 10 min in Fig. 1.

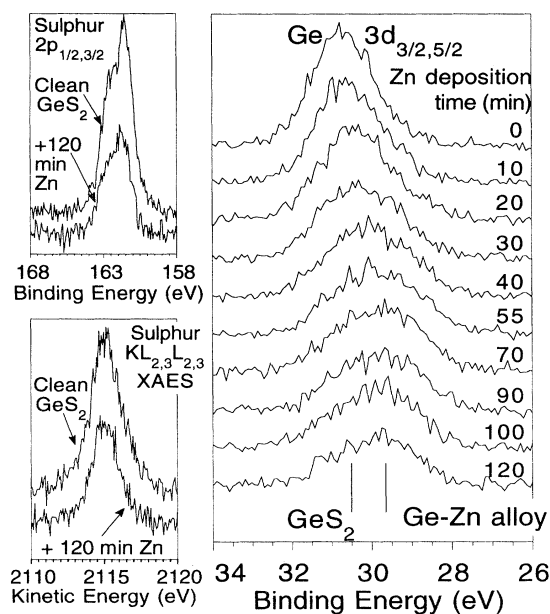


FIG. 3. The substrate $Ge\ 3d_{3/2,5/2}$ (a), $S\ 2p_{1/2,3/2}$ XPS (b), and $S\ KL_{2,3}L_{2,3}$ XAES (c) spectra as a function of Zn deposition time on a clean GeS_2 film. The Zn deposition rate in this case was $0.25\times$ that of the experiment in Fig. 1. Thus, a deposition time of 40 min here corresponds to a deposition time of 10 min in Fig. 1.

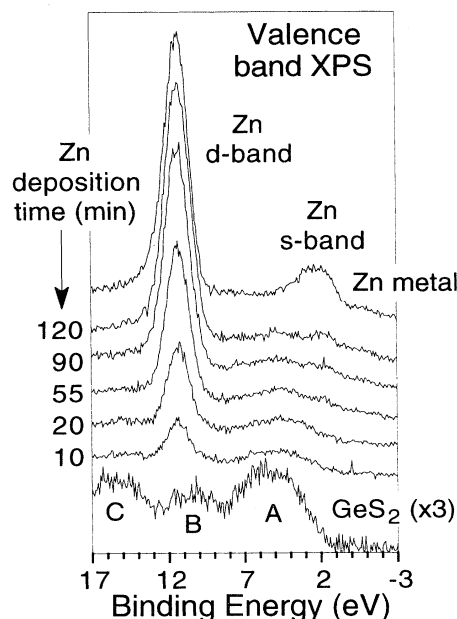


FIG. 4. The valence band XPS as a function of Zn deposition time on a clean GeS_2 film. The peaks identified as A through C in the GeS_2 spectrum are identified in the text. The Zn deposition rate in this case was $0.25\times$ that of the experiment in Fig. 1. Thus, a deposition time of 40 min here corresponds to a deposition time of 10 min in Fig. 1.

time on the clean film; the inset to Fig. 2 shows the same spectrum for Zn deposition on a GeS_2 film photo-oxidized to the saturation point. The Zn $L_3M_{4.5}M_{4.5}$ transition contains two distinct electronic contributions: a major peak consisting of the 1G and 1D transitions, and a less intense shoulder about 4 eV higher in kinetic energy attributable to the 3F transitions.^{13,14} No changes in the Zn $2p_{3/2}$ XPS peak at a binding energy (E_B) of 1021.8 eV were observed. However, Fig. 2 demonstrates the presence of two distinct chemical states during the Zn deposition. The main electronic transition ($^1G/{}^1D$) for the first of these lies at a kinetic energy (E_k) of 990.5 eV (Auger parameter, $\alpha=2012.3$ eV) at low Zn coverages, saturating at 40 min deposition time. The second chemical state appears for deposition times greater than 40 min (i.e., after the break point). Its main transition lies at $E_k=992.3$ eV and $\alpha=2014.1$ eV. In the inset, the spectra again indicate the presence of the same two chemical states except that here both appear to grow simultaneously. In neither set of spectra is there any evidence for states typical of ZnS ($E_k=989.7$ eV) or ZnO ($E_k=987.7$ eV).¹⁵

The $Ge\ 3d_{3/2,5/2}$ XPS, $S\ 2p_{1/2,3/2}$ XPS, and $S\ KL_{2,3}L_{2,3}$ XAES spectra as a function of Zn deposition time are shown in Fig. 3. The S XAES transition lies at energies above those of the primary exciting radiation, Al $K\alpha$ at 1486.6 eV, and is thus excited by the bremsstrahlung background from the x-ray source. The S spectra show no change upon Zn deposition: the chemical shifts

and Auger parameters remain typical of GeS_2 ($\alpha=2277.3$ eV). Similarly, no changes were observed during Zn deposition on the photo-oxidized film. In contrast, the Ge spectra show considerable changes upon Zn deposition. The XPS emission shifts from a E_B of 30.5 to 29.5 eV, completed by about 40 min deposition time. The Ge $L_3M_{4,5}M_{4,5}$ XAES spectrum shows a similar pattern with the peak shifting from $E_k=1142.6$ eV (typical of GeS_2) to $E_k=1144.8$ eV. The corresponding shift in Auger parameter is thus from $\alpha=1173.1$ to 1174.3 eV. On the photo-oxidized film a similar shift is observed, but with a distinct contribution from the substrate signal being observed even at Zn deposition times > 100 min.

The O $1s$ XPS spectra also demonstrate no change in chemical shift over the period of Zn deposition on a GeS_2 film photo-oxidized to the saturation point. The peak is at $E_B=530.7$ eV typical of O in the 2- oxidation state.¹⁶ The spectra do, however, demonstrate considerable attenuation, even at low Zn coverages. By 20 min deposition time, the peak area has attenuated to 0.56 of its initial value; the attenuation has reached 0.35 by 100 min Zn deposition time. Such rapid attenuation was not observed in any other of the XP or electron-excited Auger spectra.

The valence-band XPS spectrum for clean GeS_2 and for various Zn deposition times on the clean substrate are shown in Fig. 4. The GeS_2 valence spectrum consists of three bands, which have been previously characterized.¹⁷ The *A* band contains S $3p$ lone pair states at energies nearest the band gap and S $3p/\text{Ge } 4p$ binding states at lower energies. The *B* band consists mainly of Ge $4s$ states and band *C* of S $3s$ states. As Zn is deposited on the GeS_2 substrate, a peak corresponding to the Zn *d* band appears at 11.5 eV and a smaller peak corresponding to the *s* band at 2.5 eV. There is little apparent difference in the spectra before and after the break point at 40 min deposition time.

B. GeS_2 deposition on Zn

In order to shed further light on the nature of the metal/semiconductor interface, and to aid in the interpretation of the following EXAFS results, we examined the "inverse" system: GeS_2 on Zn. GeS_2 was deposited on a Zn film and the Zn $L_3M_{4,5}M_{4,5}$ (990 eV), Ge $L_3M_{4,5}M_{4,5}$ (1140 eV), and S $LM_{2,3}M_{2,3}$ (50 eV) AES intensities measured as a function of deposition time in chamber *B*. The results are shown in Fig. 5: Neither of the S or Ge uptakes demonstrate the presence of a strong break point. The S signal is also seen to grow much more rapidly than the Ge signal. This trend is also apparent in the XP spectra, with higher S:Ge ratios appearing at low deposition times. At 0.75 min, the S $2p$ (1325 eV):Ge $3d$ (1455 eV) ratio is 3.5 decreasing towards a value of 1.7 (typical of clean GeS_2 films) by 15 min deposition time. Similarly, the S XAES (2115 eV):Ge $3d$ (1455 eV) ratio is 2.0 at 0.75 min, decreasing to 0.50 at 15 min.

While the Zn $2p_{3/2}$ XPS spectra again showed no change (other than attenuation) on GeS_2 deposition, the

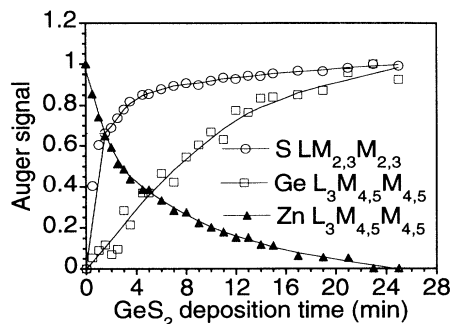


FIG. 5. The S, Ge, and Zn Auger peak-to-peak heights, as a function of GeS_2 deposition time on a Zn film.

Zn $L_3M_{4,5}M_{4,5}$ XAES spectra (Fig. 6) demonstrate the presence of three chemical states. Two of these were observed for Zn deposition on GeS_2 : the peak at $E_k=992.3$ eV attenuates throughout the deposition, while the peak at 990.5 eV maximizes at about 2 min deposition time and then attenuates. The new peak, centered at about 988 eV, is considerably weaker and is completely quenched by about 2 min deposition time.

The remaining XP spectra also show changes in chemical shift. Thus, the Ge spectra demonstrate the presence of the same two states as for Zn deposition on GeS_2 . Here, the state at $\alpha=1174.3$ eV is present at deposition times < 2 min, while after 2 min the state at $\alpha=1173.1$ eV associated with GeS_2 begins to appear, dominating the spectrum by 15 min deposition time. The S spectra are more interesting in that they also demonstrate chemical shifts, indicating a metal-S interaction in the inverse deposition mode. The S $2p_{1/2,3/2}E_B$ and S XAES E_k start out at values of 161.9 and 2115.0 eV, respectively ($\alpha=2276.9$ eV). These values shift to those typical of GeS_2 by about 2 min deposition time.

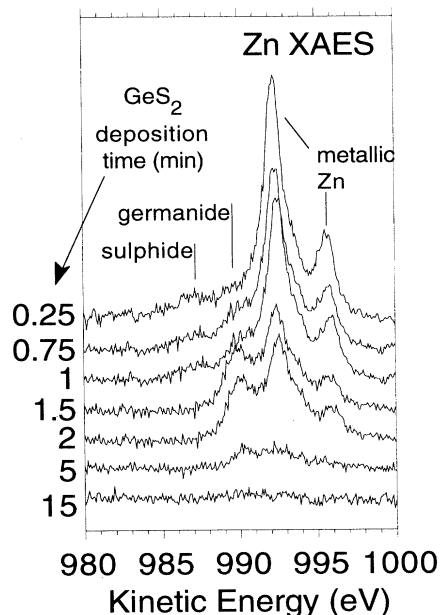


FIG. 6. The Zn $L_3M_{4,5}M_{4,5}$ XAES spectrum as a function of GeS_2 deposition time on a Zn film.

C. EXAFS

The Ge *K*-edge EXAFS spectrum and Fourier transform of an 80-Å of GeS₂ deposited on Ni foil and of the layered Zn/GeS₂ sample are shown in Fig. 7. The parameters used in fitting the spectra are given in Table I. The Zn *K*-edge EXAFS and Fourier transform for the Zn/GeS₂ sample and the ZnS and Zn foil standards are shown in Fig. 8. The relevant fitting parameters are given in Table II. An examination of the spectra and fitting parameters indicates that the Zn present in the sample has for the most part reacted with GeS₂, leading to both sulfide and germanide formation. A comparison to the crystalline standards also indicates that the sample possesses little order beyond about 3 Å.

IV. DISCUSSION

A. Zn deposition on GeS₂

We first consider the case of Zn deposition on the as-deposited GeS₂ substrate. The breakpoint in the Zn uptake data of Fig. 1 indicates a layer-by-layer growth mode on the clean CVS film, with a clear distinction between the contact layer and the metallic Zn overlayers which follow. The Zn XAES spectra in Fig. 2 are consistent with this interpretation: a contact layer state appears first and saturates at the deposition time corresponding to the break point. This is followed by the appearance of an overlayer state with an Auger parameter (2014.1 eV) typical of metallic Zn.¹⁵ A Zn Auger parameter similar to that for the contact layer (2012.3 eV) has not been previously reported in the literature. The Ge Auger parameter

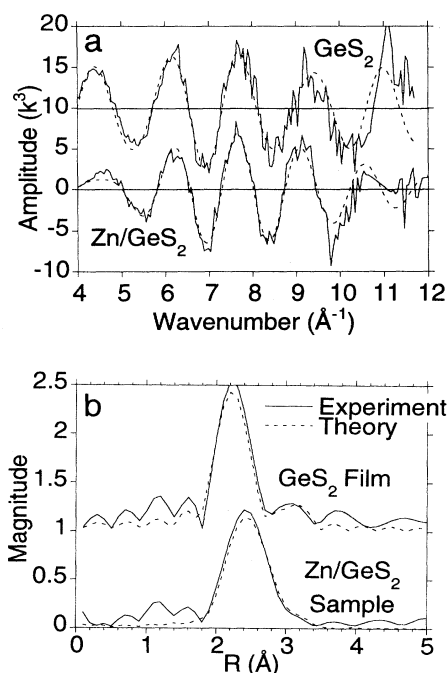


FIG. 7. The Ge *K*-edge EXAFS (a) and Fourier transform (b) for a clean GeS₂ film and the Zn/GeS₂ sample.

TABLE I. Parameters for the Ge *K*-edge EXAFS spectra.

Parameter		80-Å GeS ₂ film	Zn/GeS ₂ sample
First	<i>R</i> 1 (Å)	2.261±0.002	2.277±0.004
Shell	<i>N</i> 1	3.7±0.1	1.35±0.07
(Ge-S)	<i>A</i> 1 (Å ²)	0.0063±0.0006	0.0055±0.0001
Second	<i>R</i> 2 (Å)	N/A	2.521±0.003
Shell	<i>N</i> 2	N/A	3.1±0.1
(Ge-Zn)	<i>A</i> 2 (Å ²)	N/A	0.0129±0.0006
Third	<i>R</i> 3 (Å)	2.95±0.01	2.98±0.02
Shell	<i>N</i> 3	2.4±0.5	0.8±0.2
(Ge-Ge)	<i>A</i> 3 (Å ²)	0.021±0.003	0.017±0.005
<i>E_F</i> (eV)		-8.7±0.3	-6.0±0.3
AFAC ^a		0.75±0.02	0.71±0.02
<i>R</i> factor		39.7	35.8

^aThe amplitude factor.

and binding energy are similar to those we have previously observed for Ge in contact with Ni.¹¹ The Auger parameter shift $\Delta\alpha=1.2$ eV and chemical shift $\Delta\xi=-1.0$ eV indicate an increase in polarizability and decrease in electronegativity of the Ge environment¹⁸ consistent with Zn-Ge bond formation. The lack of any shift in the S XPS and XAES spectra is good evidence that S does not directly bond to Zn in this contact layer. The S Auger parameter for ZnS is 2276.1 eV,¹⁵ considerably different from the 2277.3 eV observed here for GeS₂.

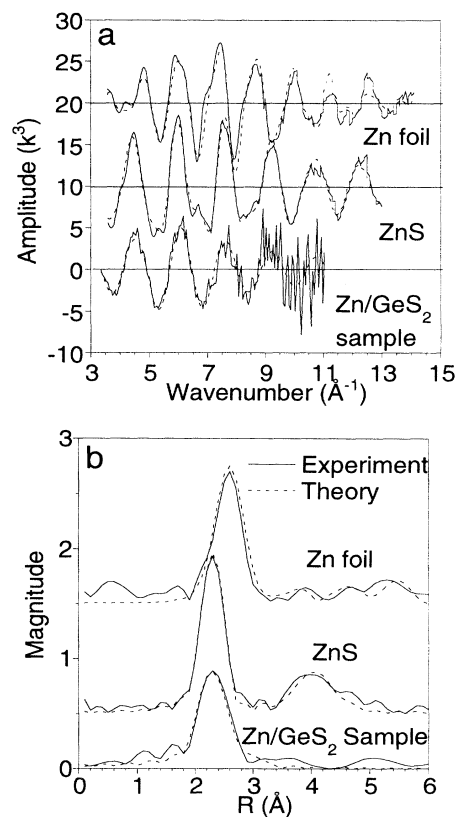


FIG. 8. The Zn *K*-edge EXAFS (a) and Fourier transform (b) for a Zn foil, ZnS, and the Zn/GeS₂ sample.

TABLE II. Parameters for the Zn *K*-edge EXAFS spectra.

Parameter		Sample 4 Zn/GeS ₂	Zn foil	ZnS
Zn-S	R (Å)	2.310±0.004		2.333±0.002
	A (Å ²)	0.014±0.001		0.0091±0.0007
	N	3.1±0.1		4
Zn-Ge	R (Å)	2.52±0.02		
	A (Å ²)	0.015±0.005		
	N	0.9±0.2		
Zn-Zn	R (Å)		2.651±0.003	3.834±0.007
	A (Å ²)		0.0226±0.0009	0.034±0.002
	N		12	12
Zn-S	R (Å)			4.41±0.02
	A (Å ²)			0.039±0.005
	N			12
Zn-Zn	R (Å)		3.83±0.01	
	A (Å ²)		0.029±0.003	
	N		6	
Zn-Zn	R (Å)		4.61±0.02	
	A (Å ²)		0.038±0.004	
	N		18	
Zn-Zn	R (Å)		4.36±0.01	
	A (Å ²)		0.011±0.002	
	N		2	
Zn-Zn	R (Å)		5.47±0.09	
	A (Å ²)		0.012±0.002	
	N		6	
AFAC ^a		0.74±0.03	0.54±0.03	0.80±0.03
E_F		2.6±0.4	1.9±0.6	0.6±0.2
R factor		38.4	34.5	34.4

^aThe amplitude factor.

The clean film S and Ge uptake data in Fig. 1 are also consistent with the growth of a Zn-Ge alloy in the contact layer. The Ge signal attenuates extremely rapidly, having been nearly quenched by the time the contact layer has been completed. This rapid quenching has been observed previously in the case of Au deposition on Ge (111) (Ref. 19), where as little as 0.5 monolayers of metal was required to quench the Ge M_1M_3V signal. This behavior was attributed to a strong electronic modification of the valence-band density of states as a Au-Ge compound was formed. A similar effect might be expected in this case if the contact layer involved a strong Ge-Zn interaction. The 150-eV S Auger-electron signal attenuates much more slowly: the 70% attenuation at the breakpoint is consistent with the overlayer thickness being some 3–5 Å thick, as judged from the universal electron attenuation curve.¹⁵ Thus, the monolayer point defined from the break in the Zn uptake curve corresponds to 3–5 Å of Ge-Zn compound.

On the photo-oxidized surface, the uptake curves in Fig. 1 indicate that, after an initial induction period, the Zn growth mode changes from layer-by-layer to island formation. *This effect is especially pronounced on the surface photo-oxidized to the saturation point:* the absence of break points and slow exponential decay of the substrate signal is indicative of a Volmer-Weber growth mode. The XP spectra indicate very little difference in the nature of the compounds formed on the photo-oxidized surface compared with the clean surface. In particular, the Zn XAES and O 1s spectra indicate that direct Zn-O bond-

ing does not occur at the interface. However, the XP spectra do confirm the Volmer-Weber growth mode as is demonstrated by the inset to Fig. 2: here, the Zn XAES signals from the Zn-Ge contact layer and metallic overlayers appear simultaneously at low deposition times. The rapid attenuation observed in the O 1s spectra also indicates that, while Zn does not bond to O sites, it does promote the removal of O from the surface region. The most likely fate for the O would be diffusion into the bulk of the CVS: our previous photo-oxidation experiments on both GeS₂⁶ and As₂S₃⁵ show that O can indeed diffuse from the surface into the bulk of these materials.

The induction period observed in Fig. 1 must correspond to the phenomena observed by Kolobov *et al.* using a quartz-crystal thickness monitor^{3,4} in Zn sticking probability experiments. From our work, judging from the value of the Zn signal observed at the end of the induction period, the crucial nucleation stage occurs within approximately the first tenth of a monolayer. An estimate of the average sticking probability during the induction period on the photo-oxidized surface can be made, by comparing the initial deposition rates with that on the clean surface. On the clean GeS₂ surface, the Zn deposition rate is about 1 ML every 10 min. On the partially photo-oxidized surface about one-tenth of a Zn monolayer has been deposited in the same time, while on the saturated photo-oxidized surface one-tenth of a monolayer is deposited in about 20 min. Thus, the initial sticking probability has been reduced by at least an order of magnitude. An inspection of the gravimetric results of

Kolobov *et al.*^{3,4} indicates a reduction of approximately two orders of magnitude in the sticking probability of Zn following photo-oxidation of As_2S_3 ; corresponding data for GeS_2 are not available. Previous work failed to recognize that changes in deposition rate are associated with changes in growth mode on the photo-oxidized films.

Indeed, the uptake curve for the partially photo-oxidized surface in Fig. 1 seems to represent a transition between the layer-by-layer growth mode on the clean surface and the Volmer-Weber growth mode on the film photo-oxidized to the saturation point. The presence of oxygen clearly tends to disrupt the formation of the Ge-Zn alloy contact layer: failure to readily form Ge-Zn bonds naturally leads to a lower sticking probability of Zn, given the high Zn vapor pressure and its lack of reactivity with both S and O on the photo-oxidized surface. The induction period then represents the period of low sticking probability when Zn atoms impinging on the surface have only a small chance of finding a reactive site. Zn, which does stick produces a Ge-Zn alloy, the formation of which drives O into the bulk of the CVS. Once a critical amount of Zn has nucleated (about 0.1 ML), islands of metal can grow on the alloy sites more easily, and the sticking probability becomes close to that on the clean surface. On surfaces which have been only partially photo-oxidized, it appears that Zn forces the diffusion of all the oxygen from the surface to form a completely reacted monolayer of Zn-Ge alloy with the subsequent growth mode identical to that on the clean film. On the saturated photo-oxidized surface, growth of the metallic Zn overlayer becomes significant before all the oxygen has been removed, leading to the Volmer-Weber growth mode.

This behavior during Zn deposition on GeS_2 is in considerable contrast to that exhibited by Ag (Refs. 6 and 9) on the clean and photo-oxidized CVS. In that case, Ag was found to interact with S sites to form Ag-S bonds and no direct Ag-Ge bonding was observed. Furthermore, differences in the growth mode on the clean and photo-oxidized films were not nearly as marked in the Ag case; no induction periods were observed, the reacted selvedge was considerably thicker and, at high metal coverages on the photo-oxidized films, there was evidence of Ag-O bonding. The previous observation of preferential oxidation of the nonchalcogen sites^{5,6,9} upon photo-oxidation demonstrates that the low sticking probability phenomenon might be a direct result of the preferential formation of Zn-Ge or Zn-As, as opposed to Zn-S, bonds when Zn is deposited on GeS_2 or As_2S_3 . It seems clear that we have proved that this is the key process that underlies this phenomenon: preferential oxidation of the nonchalcogen component of the semiconductor and a concomitant large change in the nucleation and growth mode of the Zn film. With Ag, the nonoxidized chalcogen sites are still available for bonding and, therefore, the sticking probability effect should *not* occur, as is observed.

Why oxygen tends to disrupt the formation of the Zn-Ge overlayer is still not entirely clear. Both structural and electronic effects may contribute. Our studies on the

photo-oxidation of GeS_2 (Ref. 7) indicate that on the photo-oxidized films O atoms directly replace some S atoms in the lattice forming a GeS_xO_y compound at the surface. This would not lead to gross changes in the overall geometry of the Ge site, other than a shortening of the Ge-chalcogenide bond distance. Thus, the electronic properties seem the more likely source of the effect. A consideration of the valence-band XPS spectra in Fig. 4 suggests a possible origin at least for the preferential interaction of Zn with Ge as opposed to S sites. As can be seen in Fig. 4, the Zn *d*-band valence electron density lies at the same energies as the GeS_2 *B* band. This band mainly contains contributions from Ge *s* states. In contrast, we note that the *d* bands of most transition metals (including Ag) would be expected to lie at the same energies as the GeS_2 *A* band, which contains both S lone pair and bonding states. Thus, there is considerably less possibility of Zn-S interaction than Ag-S interaction upon metal deposition on GeS_2 .

B. GeS_2 deposition on Zn

The uptake curve in Fig. 5 suggests that GeS_2 deposits on Zn in a simultaneous multilayers growth mode. The S signal saturates at about 15 min deposition time, similar to that observed for a calibration uptake for GeS_2 deposition on the Ni foil substrate. Thus, we can estimate a similar deposition rate [3–4 Å every 5 min (Ref. 6)] for GeS_2 deposition on Zn.

The initially large S to Ge intensity ratio observed in both AE and XP spectra suggest that at short deposition times the overlying film is S rich, as compared to stoichiometric GeS_2 . We have previously observed and discussed such behavior on both Ni (Ref. 11) and Ag (Ref. 6) substrates, so this would appear to be a common occurrence. The effect arises from the fact that the GeS_2 source produces both S_2 and GeS molecules in the deposition flux. The sticking probability of S_2 is sharply reduced on the initial Ge-S layer, resulting in a much more S-rich contact layer¹¹ than the overlying GeS_2 layers.

The presence of S_2 in the deposition flux clearly also has some important effects on the chemical species present at the interface. The Zn XAES spectrum indicates the presence of a third chemical state that was absent during Zn deposition on GeS_2 . This peak, at 988 eV, is indicative of Zn-S bonding at the interface, a consequence of the reaction between S_2 and Zn *which cannot occur in the "normal" system*. Further evidence for Zn-S interaction is seen from the shift in the S Auger parameter. The low coverage value of 2276.9 eV lies between those of ZnS (2276.1 eV) and GeS_2 (2277.3 eV). Thus, S at the contact layer forms Zn-S bonds. The difference between the Auger parameter observed and that for ZnS suggests that considerable interaction between Ge and S still occurs in this contact layer.

The XP spectra also indicate that the Ge-Zn compound is formed at the interface, although at a somewhat later stage than the Zn-S compound. By 5 min deposition time, much of the XP signal can be attributed to GeS_2 , indicating that overlayers of the CVS have begun to grow

on the initial contact layer. This growth mode of S-rich contact layer followed by GeS₂ overlayers has been previously observed on both Ni and S. The presence of zinc sulfide at the interface further emphasizes what we have previously observed for the Ag/GeS₂ system: that the nature of the metal/CVS interface can be strongly dependent on which order metal and CVS are deposited. This is a key point in regard to interpretation of the EXAFS results (below); i.e., the formation of Zn-S bonds is *not* an intrinsic property of Zn growth on GeS₂.

C. EXAFS

An important feature in the Zn *K*-edge spectrum is a Zn-S bond distance at 2.31 Å, which is close to that observed in the ZnS standard. There is no evidence for distances > 3 Å typical of the higher coordination shells of ZnS, demonstrating the lack of long-range order in the interlayer region. The XPS results in the previous section demonstrate that Zn-S interaction arises from the GeS₂ deposition stage of the sample preparation, *in which S₂ molecules interact with the previously deposited Zn metallic overlayer*. Thus, this result does not refute our conclusion that there is no Zn-S interaction when Zn is deposited on GeS₂. We also note that there is little evidence in the EXAFS spectrum for a first shell Zn-Zn bond distance typical of metallic Zn. This demonstrates that the sample preparation led to almost complete reaction of the Zn metal layer to form a zinc germanide and/or sulfide.

The Ge *K*-edge spectra can be fitted significantly with three coordination shells. Two of these have, with the exception of the expected reduction in coordination number, the same parameters as those observed for the first and second coordination shells of the GeS₂ film. The bond distances are typical of the high temperature form of crystalline GeS₂.¹⁹ The remaining shell is more interesting, as it indicates the presence of a Ge-Zn bond distance at 2.51 Å. This shell is also observed in the Zn *K*-edge EXAFS at the same bond distance. The coordination number for this shell is 3.1 in the Ge EXAFS, but only 0.9 in the Zn EXAFS. This suggests that the Zn-Ge compound formed is quite Zn rich. Very little structural information is available on appropriate compounds with Zn-Ge bonding as there are no well-defined alloy structures²⁰ and while a Zn₂GeS₄ compound is known, no detailed structural study appears to have been carried out.²¹

Thus, we were unable to run any standards of known structure with which to further characterize this particular shell. However, the observation of this Ge-Zn bond distance is important, since it provides strong confirmation of a principal conclusion drawn from the electron spectroscopy: that Zn will interact with Ge sites, whereas a metal such as Ag which does not show the sticking probability effect shows no evidence of Ag-Ge bonding in the EXAFS spectra.^{6,22,23}

V. CONCLUSIONS

In this section, we conclude as follows.

(1) XPS and Auger data for Zn position on clean and photo-oxidized GeS₂ directly demonstrate that chemisorption of the metal is effectively confined to the Ge sites at the surface. These act to produce the nuclei necessary for subsequent metal film growth. No significant S-Zn interaction occurs.

(2) Preferential photo-oxidation of the Ge sites strongly inhibits Ge-Zn bond formation, greatly reducing the Zn sticking probability and altering the growth mode from monolayer simultaneous monolayer to Volmer-Weber.

(3) Deposited Zn tends to drive oxygen and/or sulfur into the bulk as the contact layer evolves towards a Ge-Zn alloy.

(4) In the "inverse" case, when GeS₂ is deposited on zinc, Zn-S bonds are formed due to the presence of S₂ molecules in the impinging flux (GeS + S₂). This is important for an understanding of the EXAFS results.

(5) The EXAFS data confirm that a Zn-Ge compound is formed at the metal/semiconductor interface.

(6) Comparison with the very different behavior exhibited by Ag on clean and photo-oxidized GeS₂ strongly suggests that the proposed model for the sticking probability effect is correct.

ACKNOWLEDGMENTS

J.H.H. thanks the Association of Commonwealth Universities and British Council for providing a Commonwealth Scholarship. G.D.M. and C.H. hold a Research Fellowships at King's College and Emmanuel College, respectively. We thank the Engineering and Physical Research Council for support under Grant No. GR/J00632.

*Permanent address: Department of Chemistry, University of Keele, Keele, Staffs. ST5 5BG, United Kingdom.

†Author to whom correspondence should be addressed.

¹A. V. Kolobov and S. R. Elliott, *Adv. Phys.* **40**, 625 (1991).

²G. Pfeiffer, M. A. Paesler, and S. C. Agarwal, *J. Non-Cryst. Solids* **130**, 111 (1991).

³A. V. Kolobov and V. M. Lyubin, *Pis'ma Zh. Tekh. Fiz.* **12**, 376 (1986).

⁴G. B. Bedel'baeva, A. V. Kolobov, and V. M. Lyubin, *Philos. Mag. B* **60**, 689 (1989).

⁵A. V. Kolobov, J. P. S. Badyal, and R. M. Lambert, *Surf. Sci.* **222**, L819 (1989).

⁶J. H. Horton, K. L. Peat, and R. M. Lambert, *J. Phys. Con-*

dens. Matter **5**, 9037 (1993).

⁷J. H. Horton, C. J. Baddeley, G. D. Moggridge, R. M. Ormerod, and R. M. Lambert (unpublished).

⁸F. Stepniak, D. Rioux, and J. H. Weaver, *Phys. Rev. B* **50**, 1929 (1994).

⁹J. H. Horton, C. J. Baddeley, G. D. Moggridge, R. M. Ormerod, and R. M. Lambert (unpublished).

¹⁰C. Hardacre, R. M. Ormerod, and R. M. Lambert, *Chem. Phys. Lett.* **206**, 171 (1993).

¹¹J. H. Horton, G. D. Moggridge, R. M. Ormerod, A. V. Kolobov, and R. M. Lambert, *Thin Solid Films* **237**, 134 (1994).

¹²N. Binsted, J. W. Campbell, S. J. Gurman, and P. C. Stephenson, Computer Code EXCURV92, SERC Daresbury Labora-

- tory, Warrington, England, 1991.
- ¹³P. Weightman, *Rep. Prog. Phys.* **45**, 753 (1982).
- ¹⁴J. F. McGilp and P. Weightman, *J. Phys. C* **9**, 3541 (1976).
- ¹⁵D. Briggs and M. P. Seah, *Practical Surface Analysis Volume 1: Auger and X-ray Photoelectron Spectroscopy* (Wiley, Chichester, England, 1990).
- ¹⁶J. Jupille, P. Dolle, and M. Besacon, *Surf. Sci.* **260**, 271 (1992).
- ¹⁷T. Takahashi, Y. Haradu, and S. Hino, *Solid State Commun.* **30**, 635 (1979).
- ¹⁸C. D. Wagner, *Faraday Discuss. Chem. Soc.* **60**, 291 (1975).
- ¹⁹G. LeLay, M. Maneville, and J. J. Métois, *Surf. Sci.* **123**, 117 (1982).
- ²⁰C. Wagner, *Thermodynamics of Alloys* (Addison-Wesley, Reading, MA, 1952).
- ²¹H. Hahn and C. De Lorent, *Naturwissenschaften* **45**, 621 (1958).
- ²²J. M. Oldale, J. H. S. Rennie, and S. R. Elliott, *Thin Solid Films* **164**, 467 (1988).
- ²³J. H. Lee, A. P. Owens, and S. R. Elliott, *J. Non-Cryst. Solids* **166**, 139 (1993).